Heart Vessels (2006) 21:213–220
DOI 10.1007/s00380-005-0891-z

ORIGINAL ARTICLE

Lucio Agozzino · Pasquale Santè · Franca Ferraraccio
Marina Accardo · Marisa De Feo
Luca Salvatore De Santo · Gianantonio Nappi
Manuela Agozzino · Salvatore Esposito

Ascending aorta dilatation in aortic valve disease: morphological analysis of medial changes

Received: November 29, 2004 / Accepted: December 2, 2005

Abstract We investigated whether and how the severity of medial degeneration lesions varies along the circumference of the dilated intrapericardial aorta. Two groups of aortic wall specimens, respectively harvested in the convexity and concavity of ascending aorta in 72 patients undergoing surgery for dilatation of the intrapericardial aorta associated with aortic valve disease, were separately sent for pathology, morphometry, and ultrastructural examination. Cystic medial necrosis, fibrosis, and elastic fiber fragmentation were classified into three degrees of severity; their mean degree and morphometric findings in the convexity and in the concavity specimens were compared by paired *t*-test. Correlation between echocardiographic degree of aortic dilatation and severity of medial degeneration was assessed separately for each of the two groups of specimens. Morphologically, medial degeneration was found in all cases; a higher mean degree was found in the convexity group (2.39 ± 0.58 vs 1.44 ± 0.65 in the concavity group; $P < 0.001$). At morphometry normal smooth muscle cells in the convexity specimens were significantly reduced ($P = 0.007$); the length ($P = 0.012$) and number ($P = 0.009$) of elastic fibers reduced and increased, respectively. Moreover, in the convexity specimens a significantly smaller amount of smooth muscle cells and an increase of immunohistochemical labeling of apoptosis-associated proteins in the subintimal layer of the media was noticed. Correlation between aortic ratio and medial degeneration degree was significant in the convexity group ($P < 0.001$), but not in the concavity group ($P = 0.249$). Scanning electron microscopy analysis confirmed morphological results and allowed us to better distinguish the early pathological cavities from the microvessels, which were in the outer media in normal aorta and ubiquitous in aortitis or atherosclerosis. Electron transmission microscopy analysis showed changes in the extracellular matrix and smooth muscle cells, and these changes increased from the intima to the adventitial layer of the media. In dilated intrapericardial aorta, medial degeneration changes and expression of apoptosis-associated proteins are more marked in the ascending aorta convexity, likely due to hemodynamic stress asymmetry. Ultrastructural findings allow us to distinguish the early medial changes not yet evident on light microscopy.

Key words Aneurysm · Aortic valve · Aortic root · Medial degeneration · Electron microscopy

L. Agozzino (✉) · F. Ferraraccio · M. Accardo · S. Esposito
Department of Public Health, Section of Pathology, Second University of Naples, Via L. Armanni 5, 80138 Naples, Italy
Tel. +39-08-145-9747; Fax +39-08-145-9224
e-mail: lucio.agozzino@unina2.it

P. Santè · M. De Feo · L.S. De Santo · G. Nappi
Department of Cardio-Thoracic and Respiratory Sciences, Second University of Naples, Naples, Italy

M. Agozzino
Department of Pathology IRCCS, Policlinico S. Matteo, Pavia, Italy

S. Esposito
PhD Program in Cardiological Sciences, Second University of Naples, Naples, Italy

Introduction

The diagnosis of ascending aorta dilatation associated with aortic valve disease has been improved by new imaging techniques.[1,2] Recently, intrapericardial aorta dilatation has been differentiated into "root aneurysm" when dilatation is present proximally to the sinotubular junction and "ascending aneurysm" when it is dominant distally from the sinotubular junction;[3] in both, the most common morphological substrate is medial degeneration.

The pathogenesis of aortic wall changes underlying aneurysmal dilatation is currently an issue of debate: in particular, it has not yet been established whether medial lesions are due to primary connective tissue defects or develop secondary to hemodynamic forces, or both;[1,4] certainly ascending aorta dilatation is more frequent in congenital[5,6] or acquired aortic valve malfunction,[7] in aortic bicuspid valves,[8–10] and in some hereditary connective tissue disorders such as Marfan or Ehlers–Danlos syndrome[5]

where a spectrum of mutations in the fibrillin or type II procollagen genes were demonstrated.[11,12]

The histological changes underlying ascending aortic dilatation is Erdheim's cystic medial necrosis[13] or medial degeneration, which is characterized by a triad of noninflammatory smooth cell loss, fragmentation of elastic fibers, and accumulation of basophilic ground substance within cell-depleted areas of the medial layer of the vessel wall. These findings could either result from damage and repair events occurring in the normal aging aorta,[3,14] or be seen earlier in patients with abnormal postvalvular hemodynamics (excessive injury)[15] and in patients with connective tissue disorders (impaired repair).[5,12] Therefore, aortitis, atherosclerosis, and severe shear stress present the same histological picture of medial degeneration.[5]

New insights in aortic root anatomy and hemodynamics have recently shown a functional and structural asymmetry, which has been though to be strictly related to biomechanics.[16–18] Furthermore, aortic elastic performance plays an important role; in fact, it deteriorated in advanced age,[19] in hypertensive patients or those affected by coronary artery disease,[20] in habitual smokers,[20] in 17β-estradiol deficiency,[20] and after infusion of some drugs.[21]

Our previous studies reported the degree of aortic dilatation and the severity of histological changes in the aortic wall,[22–24] and defined the geometrical distribution of medial degeneration within the intrapericardial aorta.[25] These data have been confirmed by Westaby et al., who suggest that root dilatation begins in the noncoronary, then right coronary sinus.[26] The aim of our study was to investigate the pattern of expression of medial degeneration in a larger series to justify the choice of conservative surgical management ("waistcoat aortoplasty") of intrapericardial aortic dilatations[27] and prevent lethal complications (spontaneous rupture and dissection), also in consequence of ultrastructural findings.

Patients and methods

Between March 1999 and February 2005, aortic wall specimens were collected from 116 consecutive patients (104 men and 12 women), with a mean of age of 54.9 ± 12.1 years (range 42–75), undergoing surgery for ascending aortic dilatation with associated structurally diseased aortic valve in 70 cases (60.34%). Patients with atherosclerotic aneurysm (26 cases), aortitis (16), infective endocarditis (2), or primary connective tissue disorders (such as Marfan syndrome) were excluded from the study.

The series included 72 patients, 64 men and 8 women (M:F ratio 8:1) with a mean age of 52.1 ± 12.1 years (range: 42–75). Body surface area of patients was calculated according to the Dubois formula.[24] In 20 patients the whole ascending aorta was replaced, while in the other 52 ascending aortoplasty was performed. The aortic valve was excised and replaced with a mechanical bileaflet valve in all cases: in 34 patients it was found to be structurally diseased, while in 38 cases with no gross leaflet lesions a severe dilatation of the aortic root with severe valve incompetence was present, and no valve-sparing procedures were attempted.

Echocardiographic diagnosis

Echocardiographic measurements were performed using standard views, and by only two experienced examiners. Transvalvular flow velocities were measured using continuous-wave Doppler. Pressure gradients were then performed after correction for left ventricular outflow tract velocities using the complete Bernoulli equation. Measurements were taken under hemodynamically stable conditions; results were averaged from three subsequent measurements in sinus rhythm. Aortic valve incompetence was graded as mild if the regurgitation jet did not exceed 1 × 2 cm, moderate if it did not exceed the middle of the left ventricle and/or the tips of the papillary muscles, and severe if it exceeded the middle of the left ventricle.

Ascending aortic diameters were measured at the level of the aortic sinuses, sinotubular junction, and ascending aorta as its widest diameter from the parasternal window at end-diastole. To obtain comparable echocardiographic data, predicted aortic root dimensions were calculated by the regression formula described by Roman et al.,[28] and an aortic ratio was computed as measured diameter (maximum dilatation among sinusal level and sinotubular junction) divided by predicted diameter. Ascending aortic surgery was indicated in the case of aortic ratio reaching 1.5 or more.

Morphological study

At surgery, samples were harvested about 1 cm distal to the sinotubular junction level in the three areas corresponding to the sinuses of Valsalva (right and left in the concavity of ascending aorta and noncoronary in the convexity); specimens corresponding to the noncoronary sinus were taken from the right anterolateral wall. Also, the explanted aortic valve leaflets were sent for histology in all cases. All aortic wall specimens and valve cusp specimens were obtained by surgical excision perpendicular to the annulus.

Specimens of aortic tissue were fixed in 10% neutral buffered formalin for 24 h and then embedded in paraffin. Aortic wall specimens were oriented in cross sections, transverse to the axis of blood flow in vivo. Four-micrometer thick sections were routinely stained with hematoxylin–eosin, Weigert for elastic fibers–Van Gieson's stain, hematoxylin–orcein stain, and Alcian–Weigert stain for elastic fibers. For immunohistochemical analysis (PAP-staining according to Sternberger), 4-μm thick sections were deparaffinized, rehydrated, and predigested with trypsin for 8 min at 37°C; endogenous peroxidase was blocked with 3% H_2O_2 in a Tris-buffered saline solution for 10 min, sections were incubated for 30 min in a blocking solution, then stained with a primary monoclonal antibody against actin smooth muscle (monoclonal mouse antihuman, clone 1A4, DAKO, Glostrup, Denmark), CD95/Fas protein (monoclonal mouse antihuman, clone APO-1, DAKO), and bcl-2 protein (monoclonal mouse antihuman, clone 124, DAKO),

and polyclonal antibodies against Bax (polyclonal rabbit antihuman, A 3533 Ig fraction, DAKO) and caspase 3/CPP32 (polyclonal rabbit antihuman, A 3537 Ig fraction, DAKO), respectively. Immunohistochemistry was used to determine the density and the apoptosis of smooth muscle cells. Apoptotic cells and smooth muscle cell nuclei were counted using computer-generated image analysis (VIDAS Kontron Elektronik Zeiss, Munich, Germany).

For each specimen, histological changes of medial degeneration were evaluated according to the criteria of de Sa et al.[10] and Schlatmann and Becker[14,15]: cystic medial degeneration, defined as pooling of mucoid material; elastic fragmentation characterized by destruction of elastin lamellae; fibrosis, defined as replacement of smooth muscle cells with collagen proliferation; medionecrosis, defined as areas with apparent nuclei loss. The above-mentioned changes were ranked in three different grades: grade 1 (mild), grade 2 (moderate), and grade 3 (severe).

Morphometric analysis was performed by using two programs (RM 2100 or RM 5200) of a computer-assisted image analysis system (VIDAS Kontron Elektronik). For each specimen, five microscopic fields (final magnification ×620) were randomly selected from the external, central, and internal layers of the media (total of 15 reference areas for each specimen); the number of elastic fibers, total smooth muscle cells (normal and degenerated together), and normal smooth muscle cells alone was counted and mean values were computed. The length of elastic fibers, considering their angulation and their density per field, was also measured.

The ultrastructural study was performed using small aortic tissue samples (2 mm thick), fixed in 4% paraformaldehyde in phosphate buffer, postfixed for 1 h in 1% OsO_4, embedded in Epon 812 resin, cut in ultrathin sections (600 Å in thickness) that were mounted in slot grids and double stained with lead citrate and uranyl acetate. Selection of zones for electron microscopic analysis was made on semithin sections stained with toluidine blue. They were then examined with a Zeiss EM 902 transmission electron microscope at magnifications ranging from ×110 to ×20 000.

In 26 patients, scanning electron microscopy analysis was performed using 0.5-mm thick fragments, fixed in 10% buffered formalin at pH 7.4 and osmolarity 0.1, alcohol dehydrated, and put in Critical Point chambers in order to change the solvent with liquid CO_2 at 38°C temperature and 85 bar pressure. Following this procedure, the fragments were put in a Sputtering Device Emitech (Kent, UK) K550 chamber, emptying at 0.05 mbar pressure. A 30 mÅ thin gold coating was used in a DSM 940 Zeiss scanning electron microscope following Argon ion acceleration. Scanning electron microscope morphometric analysis was performed using the same programs and image analysis system as described above.

Statistical analysis

To evaluate differences in medial degeneration severity between the two aortic sites, degrees of medial degeneration were coded as discrete variables assigned to each specimen (two groups of values composed by the same patients), and comparisons between convexity and concavity specimens were made using the paired *t*-test. Paired *t*-test was also employed to compare morphometric findings between the two groups of specimens.

Moreover, patients were divided into three groups according to the aortic ratio (>1.7, 1.6–1.7, or <1.6). For each of the two groups of specimens the correlation between class of aortic ratio and degree of medial degeneration was assessed using the chi-square test with Yates' continuity correction.

Results

Echocardiographic and macroscopic findings

At echocardiography severe aortic valve incompetence was found in 38, stenosis in 26 (moderate in 8 and severe in 18), and mixed valve malfunction in 8 patients.

Morphologically, the ascending aorta convexity distal to the noncoronary sinus was enlarged and thinned in all cases; at transillumination, the wall was transparent in all cases. On the other hand, the ascending aorta concavity distal to the coronary sinus showed normal thickness in 62 patients, while it was slightly thinned in the other 10.

Morphological, morphometric, and immunohistochemical findings

On histologic investigation, medial degeneration was found in all cases. A more severe involvement of the convexity wall was observed in 52 patients (Fig. 1) (grade 3 vs grade 1 or 2 in 28, grade 2 vs 1 in 24) and a similar degree of involvement of both sites in 20. The mean degree of medial degeneration in convexity specimens was 2.39 ± 0.58 vs 1.44 ± 0.65 in the concavity specimens ($P < 0.001$). There was only a slight significance ($P = 0.034$) as far as the degree of concavity medial degeneration among the patients with and without structural changes was concerned.

Pathological examination of valve leaflets showed structural aortic valve disease in 34 cases: chronic rheumatic valve disease in 28 patients (6 on bicuspid valve), dystrophic calcific valve disease in 4 (2 on bicuspid valve), bicuspid aortic valve in 4, and floppy aortic valve in 2. The aortic valve was congenitally bicuspid in 14 patients of our series: 6 with chronic rheumatic valve disease, 2 with dystrophic calcific disease, 2 with floppy aortic valve, and 4 with normal valve. Eight patients with congenitally aortic bicuspid valve were allocated to a subgroup characterized by the higher degree of global medial degeneration expression. In 38 patients the valve showed no changes at morphologic examination, but it was removed because of incompetence from severe aortic root and annulus dilatation.

Morphometric analysis results are summarized in Table 1. Smooth muscle cell loss was found in 40 out of 72 patients (Fig. 2); normal smooth muscle cell density was significantly

Table 1. Morphometric analysis of aortic wall

MD changes	Mean concavity	Mean convexity	*P*
No. of smooth muscle cells	528.1 ± 183.9	433.2 ± 195.5	0.258
No. of normal smooth muscle cells	475.1 ± 182.7	272.9 ± 160.8	0.009
No. of elastic fibers	201.8 ± 92.4	369.3 ± 208.9	0.012
Minimum length of elastic fibers	0.94 ± 0.39	0.37 ± 0.21	0.001
Greatest length of elastic fibers	13.24 ± 3.1	11.22 ± 3.35	0.175
Mean length of elastic fibers	4.55 ± 2.17	2.58 ± 1.07	0.007

MD, medial degeneration

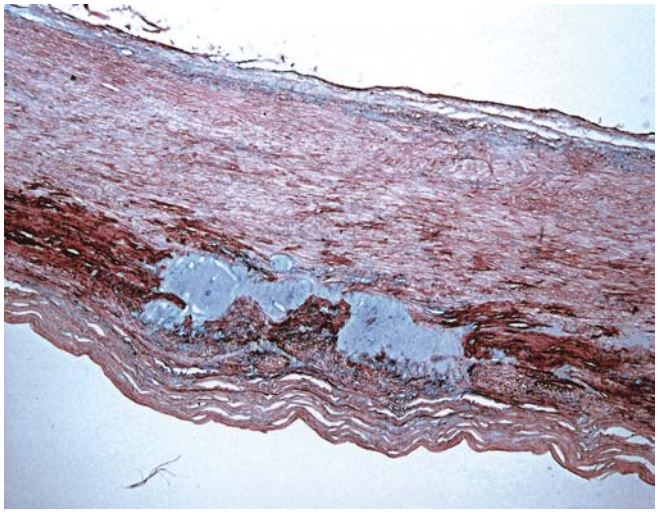

Fig. 1. Aortic wall media in a patient with severe degree medial degeneration (grade 3): widespread loss of elastic fibers with areas of total necrosis affecting more 50% of media thickness (Alcian-orceina, ×10)

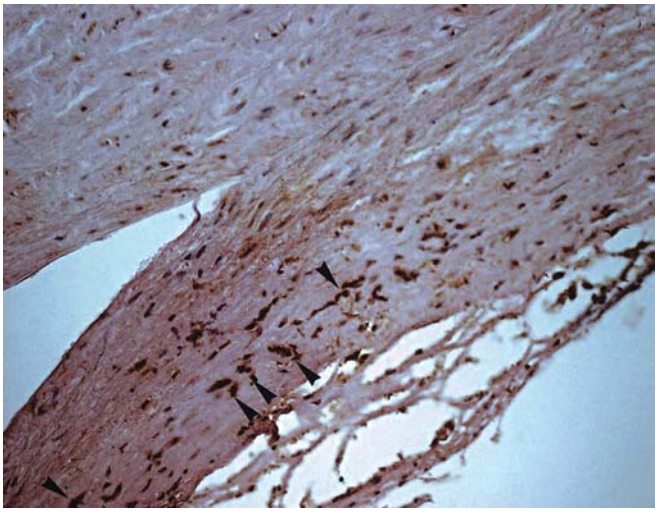

Fig. 3. Bax expression of smooth muscle cells (*arrowheads*) in a patient with severe-degree medial degeneration (PAP-staining according to Sternberger, ×20)

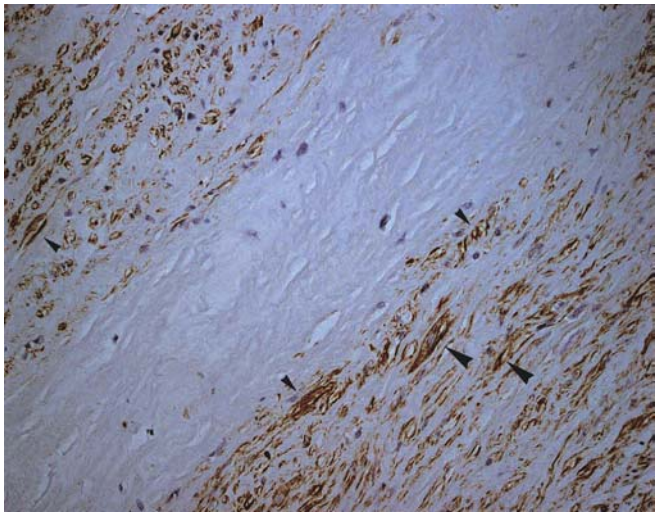

Fig. 2. Low positivity of smooth muscle cells to α-actin smooth muscle (*arrowheads*) (PAP-staining according to Sternberger, ×20)

smaller in the convexity group if it increased from the intima to the adventitial layer of the media, as also confirmed by immunohistochemical stain (P = 0.009). Elastic fiber length was reduced in 50 out of 72 patients, while their number/field was increased in these same cases. This was due to elastic fiber fragmentation. Differences between convexity and concavity specimens as to the length (P = 0.012) and number (P = 0.009) of elastic fibers were found to be statistically significant. Disruption and fragmentation were more severe, and the elastic fibers were shorter and more numerous in convexity than in concavity, in 52 patients. Morphological findings were consistent with morphometric data in 30 patients. The elastic lamellae in the aortic media of patients with bicuspid valve were severely shortened both in the concavity (3.98 ± 1.78) and convexity (2.01 ± 0.98) specimens, with increased distance among the lamellae.

On immunohistochemical analysis, smooth muscle cells showed a significant expression (P < 0.05) of bcl-2 (12.1 ± 2.7 cells/high-power field [HPF]), bax (14.8 ± 2.7 cells/HPF) (Fig. 3), caspase (15.3 ± 3.1 cells/HPF), and CD 95 (13.4 ± 1.7 cells/HPF) in the convexity of 21 of 45 patients examined when compared with that of the concavity; 16 patients had a medial degeneration of grade 3. In 17 patients (80.9%) it was more marked in convexity fragments, while in 4 it was the same in both convexity and concavity. Moreover, smooth muscle cells showed variable labeling, being marked in the subintimal layer and absent in the external layer of the media.

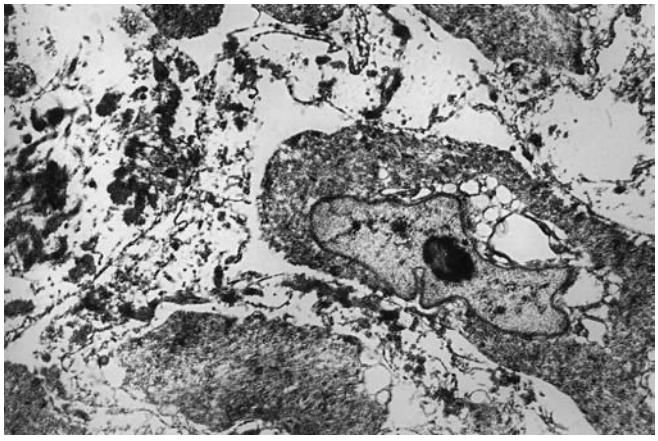

Fig. 4. Transmission electron microscopy: vacuolated cytoplasm and mitochondrial swelling in one smooth muscle cell (×4400)

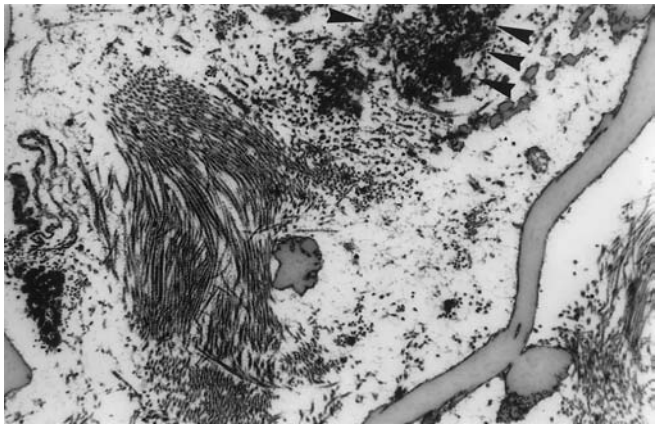

Fig. 5. Transmission electron microscopy: elastic fiber fragmentation with clusters of fibrillin (*arrowheads*) (×3000)

Ultrastructural findings

All investigated specimens at transmission electron microscopy, performed on 27 cases, showed changes in the extracellular matrix and smooth muscle cells. In fact smooth muscle cells were irregular in shape, with distorted intracellular organelles. The ones near to the pseudocysts showed degenerative changes such as hydropic change (vacuolated cytoplasm, enlarged endoplasmic reticulum, mitochondrial swelling, and cristolysis) (Fig. 4), and a decreased amount of myofilaments, sometimes with myelin figures or none at all. Nuclei of smooth muscle cells were irregular in shape. Some nuclei showed chromatin margination into sharply delineated huge masses, budding, blebbing, or apoptotic bodies.

Most of the elastin fibers were damaged, thereby composing irregular fragments. In some regions between them and the collagen fibers, numerous vesicle and pseudocyst pooling of mucoid material and thin fibrils and clusters of fibrillin (Fig. 5) were observed. These ultrastructural changes increased from the adventitial layer to the intima of the media; moreover, they were strongly marked in convexity in all cases and were consistent with morphological ones in 18 patients.

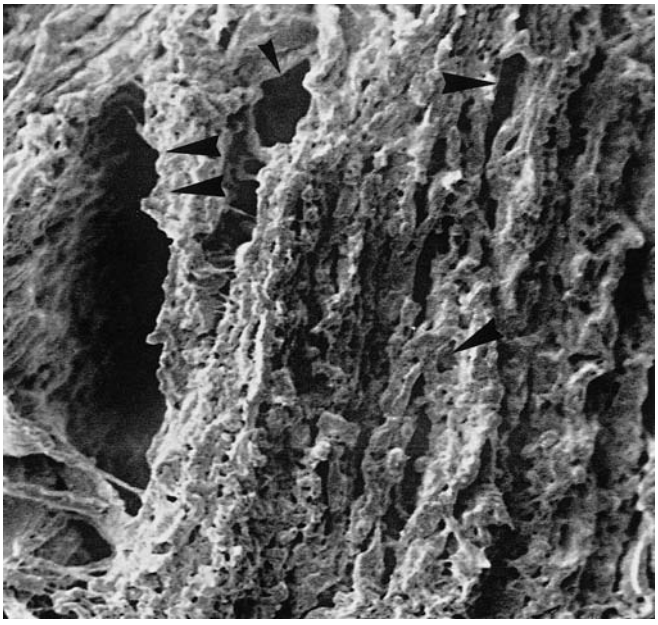

Fig. 6. Scanning electron microscopy: cavities lacking endothelium, anfractuous and lined by disorganized elastic fibers (*arrowheads*) (×1000)

Scanning electron microscopy showed a cribrose appearance at low magnification (×50–100); at high magnification (×500–2000), many cavities lacking endothelium, anfractuous and lined by elastic fibers and smooth muscle cells, were observed (Fig. 6). Such cavities had a maximum diameter of 200 μm in fragments from aortic convexity and of 100 μm in those from concavity. In the convexity an elastic fibers tridimensional disarray and diastases with development of small cavities (<2 μm) similar to the big ones were found. To evaluate the above findings, they were compared with controls taken from normal aortae.

The correlation between aortic ratio range and medial degeneration degree was found to be statistically significant only in the group of specimens corresponding to the convexity ($P < 0.001$), while the degree of aortic enlargement did not significantly correlate with the degree of involvement of the concavity ($P = 0.249$) (Table 2). The degree of medial degeneration in patients with congenitally bicuspid aortic valve was 3 vs 1 (convexity vs concavity) in two patients, 3 vs 2 in two patients, 2 vs 1 in four patients, and similar in six patients.

Discussion

A definite pattern of distribution of medial degeneration severity within the aortic wall has already been described.[25] This pattern was consistent both with the recent finding of asymmetry in the functional anatomy of the aortic root[16–18,29] and with the proposed stress origin of medial degeneration lesions.[4,14,15]

Table 2. Histological findings grouped according to the aortic ratio (column percentages and *P* values are reported)

Aortic ratio[a]	*n*	Convexity			Concavity		
		Degree 1	Degree 2	Degree 3	Degree 1	Degree 2	Degree 3
<1.6	30	8 (100%)	22 (73.3%)	0	22 (45.8%)	4 (22.2%)	0
1.6–1.7	20	0	8 (26.7%)	12 (35.3%)	18 (37.5%)	6 (33.3%)	0
>1.7	22	0	0	22 (64.7%)	8 (16.7%)	8 (44.5%)	6 (100%)
Total	72	8	30	34	48	18	6
P			<0.001			NS	

NS, not significant
[a] Measured diameter (maximum dilatation among sinusal level and sinotubular junction) divided by predicted diameter[23]

Our results confirmed the correlation between the degree of aortic dilatation and the aortic wall changes previously observed by us[22–25] and others,[30] but also added interesting information: such a correlation was found to be more significant for the aortic convexity than for the aortic concavity wall. Likely, a more severe medial degeneration could increase the risk of aortic wall dissection or rupture. Further investigations are needed to prove correlations between the extent of medial degeneration and the severity and/or the type of valve malfunction.[27]

Scanning and transmission electron microsopy analysis confirmed that the convexity changes were more marked when compared with the concavity ones. Transmission electron microscopy showed the early changes of elastic lamellae and smooth muscle cells such as dilated endoplasmic reticulum, mitochondrial swelling and cristolysis, and focal dissolution of actin and myosin, not evident on light microscopy. Some smooth muscle cells showed apoptotic changes such as chromatin margination into sharply delineated huge masses, budding, blebbing, or apoptotic bodies. Moreover, the amount of these changes increased from the adventitial layer to the intima layer of the media. Scanning electron microscopy images allowed to better distinguish the pathological cavities from the microvessels, which were in the outer media in normal aorta and ubiquitous in aortitis or atherosclerosis. The small cavities lined by fragmented elastic fibers and smooth muscle cells represent the first lesion that successively evolves in the large cavities and the pseudocysts, evident also under light microscopy. These cavities, seen only by scanning electron microscopy, are due to elastic fiber fragmentation and also exhibit a concomitant increase in mucopolysaccharides and reparative changes, such as the formation of connective tissue fibers.[14,15] Also, these cavities are bigger in the intima layer than in the adventitial one. Scanning and transmission electron microscopy are useful to identify the early changes of medial degeneration.

Congenitally bicuspid aortic valves are known to be associated with aortic cystic medial necrosis, coarctation, and congenital aortic arch abnormality.[8–10,31] A common pathogenesis of ascending aorta and aortic valve disease is postulated by Schievink and Mokri,[32] likely due to the common embryonic origin of aortic valve and ascending intrapericardial aorta. In addition, echocardiographic observations demonstrated an association of aortic dilatation with congenital aortic bicuspid valve in the absence of hemodynamic valvular abnormality.[33] Parai et al.[34] measured, by computer-aided morphometry, the severity of aortic medial degeneration associated with stenotic congenitally bicuspid and tricuspid aortic valve in patients who died shortly after aortic valve replacement, and demonstrated that aortae of congenitally bicuspid aortic valve patients had less elastic tissue than those with tricuspid valves. The aortic valve was congenitally bicuspid in 14 patients of the series; 8 patients could be allocated to a subgroup characterized by the higher degree of global medial degeneration expression. Therefore, although the numbers are too small to draw any conclusion, according to the investigations of Bechtel et al.[9] and Parai et al.,[34] it is possible to assert that patients with aortic bicuspid valve have a high degree of medial degeneration. As far as the association with congenital valvular diseases is concerned, a reduction in neuroectodermic smooth muscle cells has been shown (positive to glial fibrillar acid protein), which is likely to be involved in an abnormal development of both the aortic valve and root.[35]

Recent research has indicated that apoptosis of medial smooth muscle cells is a widespread phenomenon, responsible for mediating profound changes in arterial architecture.[36–38] The regulation of apoptosis in the aortic wall is complex, and likely to consist of multiple interacting nuclear (p53), cytoplasmic/mitochondrial (bcl-2 family), or membrane receptors (CD95/Fas, TNF) pathways, which finally activate a cascade of cysteine proteases (caspases).[39] In fact, a powerful caspase-activating system is mediated by cytokine receptors of the tumor necrosis factor family, notably fas/apo-1/CD95.[39] Our preliminary data showed a significant expression ($P < 0.05$) of bcl-2, bax, caspase, and CD95 in the smooth muscle cells of the convexity in 21 of 45 patients (46.7%) examined when compared with those of the concavity. Apoptosis was present in 76.2% of patients with grade 3 and was more marked in the internal layer of the media in the convexity (80.9%).

Degeneration and depletion of smooth muscle cells and the role of apoptosis in the disappearance of medial smooth muscle cells in the aortic wall play a key role in the development of aortic aneurysm, because smooth muscle cells participate in the matrix repair process by synthesizing extracellular protein such as collagen, elastin, and proteoglycans, and in the matrix degradation process through the release of proteinases, degrading extracellular matrix proteins when these cells change phenotype.[40] A p-

53 and bax increase in areas lacking smooth muscle cells in Marfan syndrome patients was shown; therefore apoptosis induced by wall stress could also play an important role in the pathogenesis of medial degeneration.[36,37] In our series, smooth muscle cells displayed moderate intrinsic expression of the apoptosis–promoting factor Bax, apoptosis inhibitor bcl-2, the CD-95 receptor, and the activated form of caspase-3/CPP32 in the subintimal layer, while it was rare or absent in the external layer of the media. These data support the hypothesis that wall stress also plays an important role in the induction of apoptosis and in the formation of aneurysms, chiefly in the subintimal layer.[36,37,41] However, the absence of immunohistochemical labeling of apoptosis-associated proteins or unspecific staining, in some cases, may also be due likely to fixation, so it needs to be confirmed by further procedures such as TUNEL assay and DNA electrophoresis.[42]

Our morphological results are consistent with previous anatomofunctional observations, showing an asymmetrical involvement of the proximal aorta in medial degeneration lesions, a marked induction of apoptosis in the aorta convexity, and a decrease in smooth muscle cell density. Identifying the structures of the involved proteins could be an enlightening advance in the debate on the pathogenesis of the dilatation of the intrapericardial aorta, and could also relate asymmetry in biomechanics to asymmetry in histological changes.

Acknowledgments Supported by grant MURST 2004: "Morphological diagnostics (immunohistochemical, biomolecular and ultrastructural) of cardiovascular surgery infections in heart transplantation and in valvular and prothesic pathologies" and by MIUR 2001 grant for Research Center for Cardiovascular Diseases.

References

1. Guiney TE, Davies MJ, Parker DJ, Leech GJ, Leatham A (1987) The aetiology and course of isolated severe aortic regurgitation: a clinical, pathological and ecocardiographic study. Br Heart J 58: 358–368
2. Awadalla HM, Salloum JG, Andereson HV (2004) Three-dimensional reconstruction of a rotational abdominal aortogram showing a renal artery aneurysm. Heart Vessels 19:101–102
3. Ohtsubo S, Itoh T, Furukawa K, Rikitake K, Okazaki Y, Natsuali M (2002) Geometrical difference between an ascending aneurysm and a root aneurysm in valve sparing operations. Jpn J Thorac Cardiovasc Surg 50:59–65
4. Barnett MG, Fiore AC, Vaca KJ, Milligan TW, Barner HB (1995) Tailoring aortoplasty for repari of fusiform ascending aortic aneurysms. Ann Thorac Surg 59:497–501
5. Bonderman D, Gharehbaghi-Schnell E, Wollenek G, Maurer G, Baumgartner H, Lang IM (1999) Mechanisms underlying aortic dilatation in congenital aortic valve malformation. Circulation 99:2138–2143
6. Keane MG, Wiegers SE, Plappert T, Pochettino A, Bavaria J, Sutton M (2000) Bicuspid aortic valves are associated with aortic dilatation out of proportion to coexistent valvular lesions. Circulation 102:III-35
7. Mueller XM, Tevaearai HT, Genton CY, Hurni M, Ruchat P, Fischer AP, Stumpe F, von Segesser LK (1997) Drawback of aortoplasty for aneurysm of the ascending aorta associated with aoritc valve disease. Ann Thorac Surg 63:762–766
8. Bauer M, Pasic M, Meyer R, Goetze N, Bauer U, Siniawski H, Hetzer R (2002) Morphometric analysis of aortic media in patients with bicuspid and tricuspid aortic valve. Ann Thorac Surg 74:58–62
9. Bechtel MJF, Noack F, Sayk F, Erasmi AW, Bartels C, Sievers HH (2003) Histopathological grading of ascending aortic aneurysm: comparison of patients with bicuspid versus tricuspid aortic valve. J Heart Valve Dis 12:54–59
10. de Sa M, Moshkovitz Y, Butany J, David TE (1999) Histologic abnormalities of the ascending aorta and pulmonary trunk in patients with bicuspid aortic valve disease: clinical relevance to the Ross procedure. J Thorac Cardiovasc Surg 118:588–594
11. Arbustini E (1998) Three novel mutations in the fibrillin gene (FBN1) in Marfan syndrome patients. Eur J Hum Genet 6:60
12. Francke U, Berg MA, Tynan K, Breen T, Liu W, Aoyama T, Gasner C, Miller DC, Furthmayr H (1995) A Gly I 127Ser mutation in an EGF-like domain of the fibrillin-1 gene is a risk factor for ascending aortic aneurysm and dissection. Am J Hum Genet 56: 1287–1296
13. Erdheim J (1929) Medionecrosis aortae idiopathica. Virchows Arch 273:454–479
14. Schlatmann TJ, Becker AE (1977) Histologic changes in the normal aging aorta: implications for dissecting aortic aneurysm. Am J Cardiol 39:13–20
15. Schlatmann TJ, Becker AE (1977) Pathogenesis of dissecting aortic aneurysm of the aorta. Comparative histopathologic study of significance of medial changes. Am J Cardiol 39:21–26
16. Grande KJ, Cochran RP, Reinhal PG, Kunzelman KS (1998) Stress variations in the human aortic root and valve: the role of anatomic asymmetry. Ann Biomed Eng 26:534–545
17. Choo SJ, McRae G, Olomon JP, St. George G, Davis W, Burleson-Bowles CL, Pang D, Luo HH, Vavra D, Cheung DT, Oury JH, Duran CM (1999) Aortic root geometry: pattern of differences between leaflets and sinuses of Valsalva. J Heart Valve Dis 8:407–415
18. Grande KJ, Cochran RP, Reiinhall PG, Kunzelman KS (2000) Mechanism of aortic valve incompetence: finite element modeling of aortic root dilatation. Ann Thorac Surg 69:1851–1857
19. Okamoto RJ, Wagenseil JE, De Long WR, Peterson SJ, Kouchoukos NT, Sundt TM 3rd (2002) Mechanical properties of dilated human ascending aorta. Ann Biomed Eng 30:624–635
20. Stefanadis C, Dernellis J, Toutouzas P (1999) Mechanical properties of the aorta determined by the pressure-diameter relation. Pathol Biol 47:696–704
21. Hayashi H, Kawamata H, Ichikawa K, et al. (2004) Rupture of a thoracic aortic aneurysm: a rare adverse reaction following systemic tissue plasminogen activator infusion. Heart Vessels 19:42–44
22. Cotrufo M, Santo LS, Esposito S, Renzulli A, Della Corte A, De Feo M, Marra C, Agozzino L (2001) Asymmetric medial degeneration of the intrapericardial aorta in aortic valve disease. Int J Cardiol 81:37–41
23. Bellitti R, Caruso A, Festa M, Mazzei V, Iesu S, Falco A, Cotrufo M, Agozzino L (1985) Prolapse of the "floppy" aortic valve as a cause of aortic regurgitation. A clinico-morphologic study. Int J Cardiol 9:399–410
24. Agozzino L, De Vivo F, Falco A, De Luca Tupputi Schinosa L, Cotrufo M (1994) Non-inflammatory aortic root disease and floppy aortic valve as cause of isolated regurgitation: a clinico-morphologic study. Int J Cardiol 45:129–134
25. Agozzino L, Ferraraccio F, Esposito S, Trocciola A, Parente A, Della Corte A, De Feo M, Cotrufo M (2002) Medial degeneration does not involve uniformly the whole ascending aorta: morphological, biochemical and clinical correlation. Eur J Cardiothorac Surg 21:675–682
26. Westaby S, Saito S, Anastasiadis K, Moorjani M, Jin XY (2002) Aortic root remodelling in atheromatous aneurysms: the role of selected sinus repair. Eur J Cardiothorac Surg 21:459–464
27. Cotrufo M, Della Corte A, De Santo LS, De Feo M, Covino FE, Dialetto G (2003) Asymmetric medial degeneration of the ascending aorta in aortic valve disease: a pilot study on the surgical management. J Heart Valve Dis 12:127–133
28. Roman MJ, Devereux RB, Kramer-Fox R, O'Laughlin J (1989) Two-dimensional echocardiographic aortic root dimensions in normal children and adults. Am J Cardiol 64:507–512

29. Redaelli A, Di Martino E, Gamba A, Procopio AM, Fumero R (1997) Assessment of the influence of the compliant aortic root on aortic valve mechanics by means of a geometrical model. Med Eng Phys 19:696–710
30. Guiney T, Leech G, Davies MJ, Wilson A, Parker J, Leatham A (1981) Non-inflammatory aortic root disease: an important cause of aortic regurgitation. Ecocardiographic and histologic correlation. Am J Cardiol 47:425
31. Niwa K, Perloff JK, Bhuta SM, Laks H, Drinkwater DC, Child JS, Miner PD (2001) Structural abnormalities of great arterial walls in congenital heart disease: light and electron microscopic analyses. Circulation 103:393–400
32. Schievink WI, Mokri B (1995) Familial aorto-cervicocephalic arterial dissections and congenitally bicuspid aortic valve. Stroke 26:1935–1940
33. Pachulski RT, Weinberg AL, Chan KL (1991) Aortic aneurysm in patients with functionally normal or minimally stenotic bicuspid aortic valve. Am J Cardiol 67:781–782
34. Parai JL, Masters RG, Walley VM, Stinson WA, Veinot JP (1999) Aortic medial changes associated with bicuspid aortic value: myth or reality? Can J Cardiol 15:1233–1238
35. Kirby ML, Gale TF, Stewart DE (1983) Neural crest cells contribute to normal aorticopulmonary septation. Science 220:1059–1061
36. Ihling C, Szombathy T, Nampoothiri K, Haendeler J, Beyersdorf F, Uhl M, Zeiher AM, Schaefer HE (1999) Cystic medial degeneration of the aorta is associated with p-53 accumulation, Bax upregulation, apoptotic cell death, and cell proliferation. Heart 82:286–293
37. Lopez-Candales A, Holmes DR, Liao S, Scott MJ, Wickline SA, Thompson RW (1997) Decreased vascular smooth muscle density in medial degeneration of human abdominal aortic aneurysms. Am J Pathol 150:993–1007
38. Bennett MR (1999) Apoptosis of vascular smooth muscle cells in vascular remodeling and atherosclerotic plaque rupture. Cardiovasc Res 41:361–368
39. Lesauskaite V, Tanganelli P, Sassi C, Neri E, Diciolla F, Ivanoviene L, Epistolato MC, Ralinga AV, Alessandrini C, Spina D (2001) Smooth muscle cells of the media in the dilatative pathology of ascending thoracic aorta: morphology, immunoreactivity for osteopontin, matrix metalloproteinases, and their inhibitors. Hum Pathol 32:1003–1011
40. Schmid FX, Bielenberg K, Holmer S, Lehle K, Djavidani B, Prasser C, Wiesenack C, Birnbaum D (2004) Structural and biomolecular changes in aorta and pulmonary trunk of patients with aortic aneurysm and valve disease: implications for the Ross procedure. Eur J Cardiothorac Surg 25:748–753
41. Rowe VL, Stevens SL, Reddick TT, Freeman MB, Donnell R, Carroll RC, Goldman MH (2000) Vascular smooth muscle cell apoptosis in aneurysmal, occlusive, and normal human aortas. J Vasc Surg 31:567–576
42. Saraste A, Pulkki K (2000) Morphologic and biochemical hallmarks of apoptosis. Cardiovasc Res 45:528–537